

76

1111.1-39

JUN 29 1936

~~Copy~~

Library L.M.A.L.

TECHNICAL MEMORANDUMS

NATIONAL ADVISORY COMMITTEE FOR AERONAUTICS

No. 796

CONTRIBUTION TO THE PROBLEM OF AIRFOILS

SPANNING A FREE JET

By J. Stüper

Luftfahrtforschung

Vol. XII, No. 8, December 25, 1935

Verlag von R. Oldenbourg, München und Berlin

Washington
June 1936

1.1

1.2.1.1

9.2.1

1



3 1176 01441 1715

NATIONAL ADVISORY COMMITTEE FOR AERONAUTICS

TECHNICAL MEMORANDUM NO. 796

CONTRIBUTION TO THE PROBLEM OF AIRFOILS

SPANNING A FREE JET*

By J. Stüper

SUMMARY

After a brief discussion of the work done up to now on an unwarped wing of constant chord spanning a free jet, the computation of the circulation and lift distribution for different forms of warped wings spanning rectangular and circular jets was carried out. The computed values are compared with test values and the agreement is found to be good. The effect of placing the wing eccentrically is slight and may be applied as a correction factor to the data obtained for wing placed in middle of jet.

INTRODUCTION

1. The problem of the airfoil spanning a free jet has in recent times assumed great practical importance for the following reasons:

In the investigation of very large models in the wind tunnel, the wings project beyond the boundary of the free jet and it is desirable to know the effect of this arrangement on the measurements. Up to the present time such investigations were conducted on models only at zero or very small lift since the jet effect could not quantitatively be determined.

2. With the present-day mode of side arrangement of the engines in multiengined aircraft, it is of practical interest to know the effect of the propeller slipstream on the part of the wing that intercepts it. The problem is of particular importance in connection with the investiga-

*"Beitrag zum Problem des durch einen Freistrahls hindurchgesteckten Tragflügels." Luftfahrtforschung, vol. 12, no. 8, pp. 267-281, December 25, 1935.

tions for longitudinal stability. Our present treatment, however, does not attack the complete problem of propeller wash, since we have assumed the air outside the jet boundary to be still air whereas in fact the air outside the propeller slipstream has velocity.

3. The free-jet type of turbines use vanes that cut across a free jet. Several investigators have considered this problem. The tests have been limited to rectangular wings without warping. For practical application, however, the case of a warped wing spanning a free jet is of particular importance. The solution will also throw light on the effect of spiral motion of the jet, which effect is of greatest significance in connection with the relation between propeller slipstream and mode of engine mounting.

I. PREVIOUS WORK ON THIS SUBJECT

In his second contribution to wing theory (reference 2), Prandtl indicates a method for obtaining quantitative relations in the case of a wing spanning a circular jet. For the circulation around any section of the airfoil, he proposes a series of odd powers of $\frac{R^2 - x^2}{R^2 + x^2}$ where R is the radius of the jet and x the ordinate across the span

$$\Gamma(x) = a_1 \frac{R^2 - x^2}{R^2 + x^2} + a_3 \left(\frac{R^2 - x^2}{R^2 + x^2} \right)^3 + a_5 \left(\frac{R^2 - x^2}{R^2 + x^2} \right)^5 + \dots$$

This series satisfied the "image" condition for the circular jet: $-f(R^2/x) = f(x)$ and vanishes at the boundary. K. Pohlhausen (see reference 2, p. 56) has worked through the computations using the first two members of the series and determined the coefficients for the case of minimum drag at given lift.

In a previous paper (reference 3) the author has computed the circulation and drag distribution for the case of an unwarped wing of constant chord, spanning the middle of a jet of rectangular or circular section. The solution was obtained by the method of images. The constant geometric incidence angle was represented by a Fourier series, and the distribution of the circulation by a similar series whose coefficients were, for the present, undetermined. The downward induced velocity at any section of the wing

could similarly be represented by a Fourier series. By comparing corresponding terms of the several series the unknown coefficients could then be determined. In the case of rectangular jet sections the sums of the series could be determined exactly, and in the case of a circular section a sufficient number of coefficients could be computed. These computations could be tested by experiment.

Pistolessi (reference 4) in his work, considers the problem of a wing spanning a circular jet. He starts with the Prandtl function, setting

$$\frac{R^2 - x^2}{R^2 + x^2} = \sin \phi$$

and develops

$$\Gamma = V \sum_1^{\infty} a_n \sin n \phi$$

He considers the case of an unwarped wing of constant chord as well as the problem of minimum drag.

Glauert (reference 5) determines the distribution of the circulation for a wing placed in a circular jet by the application of the trigonometric methods of Glauert-Munk-Lotz. He carries out the computations for a cylindrical wing. Glauert's investigations, although published in 1934, appear to have been conducted in 1932, since he is unacquainted with the work of Pistolessi and the author.

There is still to be mentioned the experimental work of Blenk and Fuchs (reference 6) which, however, is of a qualitative nature only. A comparison of the three methods of Glauert, Pistolessi, and Stüper is shown in figure 1, representing the circulation of a wing spanning a jet of circular section, the ratio R/t (where t is the chord) being 3.125. Glauert used four terms of his series, Pistolessi three terms, while the author carried through the computations to eleven terms. A fundamental difficulty in the series development used should here be pointed out. The singularity at the boundary of the jet requires that

$$\left. \frac{d\Gamma(x)}{dx} \right|_{x=R} = \infty$$

Now in the Prandtl development $\frac{d}{dx} \frac{R^2 - x^2}{R^2 + x^2} = \frac{1}{R}$ for $x = R$,

so that to obtain the above condition a large number of terms is necessary so that sufficient accuracy may be assured. A similar difficulty came up in the choice of the variables by Pistolessi and the author. This fact made it necessary in our previous work to use as many as 11 terms in spite of the very laborious computations involved. In the series employed by Glauert, the first term represents elliptical distribution of circulation, so that the normal rate of decrease at the jet boundary is already contained in the development. For comparison, the circulation distribution for a square jet (length of edge $2R$) is also shown. It is seen that there is very little deviation from the circular jet distribution obtained by Glauert. It will be shown farther on, however, that the circulation depends to a certain extent on the form of cross section of the jet. It is probable that the unevenness in the distribution curve of Pistolessi would be smoothed out by the addition of more terms.

A comparison of the theoretical results with test data is shown in figures 2 and 3. Figure 2 shows the lift distribution obtained from pressure-distribution measurements, along the wing span across the circular jet ($R/2 = 2$) (indicated by small circles), while the dotted and continuous curves give the computed values of Glauert and the author, respectively (reference 3). Pistolessi's work could not be included here since his computations were carried out for one aspect ratio only. Figure 3 shows the theoretical and experimental variation of $dc_a/d\alpha$, described in the second part of this paper.

II. THEORY

Up to the present time calculations were performed only on rectangular wings that were not twisted or warped. In order to make the theory applicable in practice, it is necessary to extend it to more general wing shapes. Of particular interest is the application to the case of a warped wing spanning a free jet. The solution of this problem also throws light on the effect of angular deflection of the jet (spiral flow) on the wing, such as occurs in the case of propeller slipstream. This motion affects the wing chiefly through a change in the relative velocity, so that the problem could be treated as if the jet were free from rotation and the wing were warped correspondingly. The amount of the warping could be determined from the jet deflection and velocity.

1. Warped Airfoil of Constant Chord Spanning
a Free Jet of Rectangular Cross Section

When a warped wing is projected across a rectangular free jet (height h , width l), the condition of the free boundary could be determined as usual by the method of images. The condition requires that no additional velocity components be created at the jet boundary by the wing. This condition is generally fulfilled by assuming the fluid to be infinite in extent and making the velocity components created by the wing at the free boundary, vanish by combining them with properly chosen additional velocity components. The effect of these additional velocity components on the wing is the effect of the free boundary.

If the angle of attack of a wing is periodically varied in such a manner that

$$\alpha(x) = -\alpha(2l-x) \quad (\text{fig. 4})$$

it is easily seen that the condition is fulfilled at the planes

$$x = 0, \pm l, \pm 2l, \pm 3l, \text{ etc.}$$

The angle of attack may be given by a Fourier series:

$$\alpha(x) = \alpha_0 \sum_1^{\infty} b_n \sin n \pi \frac{x}{l}$$

α_0 is the value of α for $x = 0$, the coefficients b_n are determined by harmonic analysis of the given warping. If we now construct a wing grating so that wings of the form described are placed at

$$z = 0, \pm h, \pm 2h, \pm 3h, \dots (\text{fig. 5})$$

there will be no induced velocities in the stream direction in the planes

$$z = \pm h/2, \pm 3h/2, \pm 5h/2, \dots$$

For each wing element there is a corresponding element giving an equal but oppositely directed induced velocity, so that the resultant vanishes. In this manner the jet

condition is fulfilled. The downward velocity at the wing induced by this system is (see reference 3, p. 341):

$$w(x) = \frac{1}{4h} \int_{-\infty}^{\infty} \frac{d\Gamma(x_1)}{dx_1} \coth \frac{\pi}{h} (x - x_1) dx_1$$

We now set

$$\Gamma(x) = \Gamma_0 \sum_1^{\infty} a_n \sin n \pi \frac{x}{l}$$

where the coefficients are as yet undetermined with

$$\Gamma_0 = \frac{c V t \alpha_0}{2}$$

($c = \frac{dC_{a\alpha}}{d\alpha}$, $V = \text{blower velocity}$, $t = \text{chord}$).

Then

$$w(x) = \Gamma_0 \sum_1^{\infty} \int_{-\infty}^{\infty} \frac{a_n n \pi}{4h l} \coth \frac{\pi}{h} (x - x_1) \cos n \pi \frac{x_1}{l} dx_1$$

After a brief computation, we obtain

$$w(x) = \Gamma_0 \sum_1^{\infty} \frac{a_n n \pi}{4 l} \frac{e^{-\frac{n}{h} \frac{\pi}{l}} + 1}{e^{-\frac{n}{h} \frac{\pi}{l}} - 1} \sin n \pi \frac{x}{l}$$

In the well-known equation from airfoil theory

$$\Gamma(x) = \frac{c V t}{2} \left[\alpha(x) - \frac{w(x)}{V} \right]$$

we substitute the Fourier series for $\Gamma(x)$, $\alpha(x)$ and $w(x)$. Comparing coefficients, we obtain:

$$a_n = \frac{b_n}{n \frac{h}{l} \pi} \quad \text{with} \quad \frac{8 l}{c t \pi} = \lambda$$

$$1 + \frac{n}{\lambda} \frac{e^{-\frac{n}{h} \frac{\pi}{l}} + 1}{e^{-\frac{n}{h} \frac{\pi}{l}} - 1}$$

As an example, the distribution of circulation was computed for a wing spanning a rectangular free jet. The warping for this wing is shown in figure 6, with

$$b_n = \frac{2}{\pi n}$$

Figure 7 shows the circulation for different aspect ratios, figure 8 gives the circulation as a function of λ , while table I gives the computed values.

TABLE I

λ	$x/l =$			
	0.0625	0.125	0.25	0.375
1	0.182	0.216	0.190	0.108
2	.295	.341	.280	.150
3	.371	.423	.329	.174
4	.435	.474	.364	.188
5	.483	.514	.389	.197
6	.518	.545	.406	.205
7	.549	.569	.420	.209
8	.575	.589	.429	.213
9	.597	.606	.438	.216
∞	.875	.750	.500	.250

2. Warped Wing with Variable Chord Spanning

a Rectangular Free Jet

If the wing, in addition to being warped, has variable chord, it is necessary to have the chord vary periodically as well as the angle of attack and in such a manner that $t_x = t(2l-x)$, as indicated in figure 9. The chord $t(x)$ is developed into a Fourier series:

$$t(x) = t_0 \sum_0^{\infty} b_m \cos m \pi \frac{x}{l} \quad t_0 = t \quad \text{for } x = 0$$

Furthermore, we have:

$$\alpha(x) = \alpha_0 \sum_1^{\infty} \beta_p \sin p \pi \frac{x}{l}$$

Setting

$$\Gamma(x) = \Gamma_0 \sum_1^{\infty} a_n \sin n \pi \frac{x}{l} \quad \left(\frac{c V t_0 \alpha_0}{2} = \Gamma_0 \right)$$

we obtain:

$$w(x) = \Gamma_0 \sum_1^{\infty} \frac{a_n \cdot n \pi}{4l} \frac{e^{n \pi \frac{h}{l}} + 1}{e^{n \pi \frac{h}{l}} - 1} \sin n \pi \frac{x}{l}$$

The coefficients b_m and β_p are known from the harmonic analysis of the angle of attack and chord.

If we substitute the above relations in the equation

$$\Gamma(x) = \frac{c V}{2} t(x) \left[\alpha(x) - \frac{w(x)}{V} \right]$$

we obtain:

$$\sum_{n=1}^{\infty} a_n \sin n \pi \frac{x}{l} = \sum_{m=0}^{\infty} \sum_{p=1}^{\infty} b_m \beta_p \cos m \pi \frac{x}{l} \sin p \pi \frac{x}{l} - \frac{ct\pi}{8l} \sum_{n=1}^{\infty} \sum_{m=0}^{\infty} a_n b_m n \frac{e^{n \pi \frac{h}{l}} + 1}{e^{n \pi \frac{h}{l}} - 1} \sin n \pi \frac{x}{l} \cos m \pi \frac{x}{l}$$

and putting $\frac{8l}{ct\pi} = \lambda$ and $n \frac{e^{n \pi \frac{h}{l}} + 1}{e^{n \pi \frac{h}{l}} - 1} = \gamma_n$

there results:

$$\begin{aligned} & \sum_{n=1}^{\infty} a_n \sin n \pi \frac{x}{l} \\ &= \frac{1}{2} \sum_{m=0}^{\infty} \sum_{p=1}^{\infty} b_m \beta_p \left[\sin (p+m) \pi \frac{x}{l} + \sin (p-m) \pi \frac{x}{l} \right] \\ &- \frac{1}{2\lambda} \sum_{m=0}^{\infty} \sum_{n=1}^{\infty} a_n \gamma_n b_m \left[\sin (n+m) \pi \frac{x}{l} + \sin (n-m) \pi \frac{x}{l} \right] \end{aligned}$$

If we compare the coefficients of corresponding terms, the following set of equations for the unknown coefficients are obtained, solved by the method of "iteration."

$$a_1 \left(1 + \frac{\gamma_1 b_0}{\lambda} - \frac{\gamma_1 b_2}{2\lambda} \right) = \frac{1}{2} \left[\beta_1 b_0 + \beta_1 (b_0 - b_2) + \beta_2 (b_1 - b_3) + \beta_3 (b_2 - b_4) + \dots \right] \\ - \frac{1}{2\lambda} \left[a_2 \gamma_2 (b_1 - b_3) + a_3 \gamma_3 (b_2 - b_4) + a_4 \gamma_4 (b_3 - b_5) + \dots \right]$$

$$a_2 \left(1 + \frac{\gamma_2 b_0}{\lambda} - \frac{\gamma_2 b_4}{2\lambda} \right) = \frac{1}{2} \left[\beta_2 b_0 + \beta_1 (b_1 - b_3) + \beta_2 (b_0 - b_4) + \beta_3 (b_1 - b_5) + \dots \right] \\ - \frac{1}{2\lambda} \left[a_1 \gamma_1 (b_1 - b_3) + a_3 \gamma_3 (b_1 - b_5) + a_4 \gamma_4 (b_2 - b_6) + \dots \right]$$

$$a_3 \left(1 + \frac{\gamma_3 b_0}{\lambda} - \frac{\gamma_3 b_6}{2\lambda} \right) = \frac{1}{2} \left[\beta_3 b_0 + \beta_1 (b_2 - b_4) + \beta_2 (b_1 - b_5) + \beta_3 (b_0 - b_6) + \dots \right] \\ - \frac{1}{2\lambda} \left[a_1 \gamma_1 (b_2 - b_4) + a_2 \gamma_2 (b_1 - b_5) + a_4 \gamma_4 (b_1 - b_7) + \dots \right]$$

$$a_4 \left(1 + \frac{\gamma_4 b_0}{\lambda} - \frac{\gamma_4 b_8}{2\lambda} \right) = \frac{1}{2} \left[\beta_4 b_0 + \beta_1 (b_3 - b_5) + \beta_2 (b_2 - b_6) + \beta_3 (b_1 - b_7) + \dots \right] \\ - \frac{1}{2\lambda} \left[a_1 \gamma_1 (b_3 - b_5) + a_2 \gamma_2 (b_2 - b_6) + a_3 \gamma_3 (b_1 - b_7) + \dots \right]$$

N.A.C.A. Technical Memorandum No. 796

3. Warped Wing of Constant Chord Spanning a Free Jet of Circular Cross Section

The problem of the cylindrical wing spanning a circular jet was solved in our previous paper by conformal transformation of the circle into a strip (reference 3)[#], p. 344. The jet condition could then be fulfilled as usual by the method of images. In the plane of the strip (ξ - η plane), the equation to be satisfied is:

$$\frac{\Gamma(\xi)}{\Gamma_\infty} \frac{\pm 1}{1 + |\sin \xi|} = \frac{\pm 1}{1 + |\sin \xi|} - \frac{c t}{2\Gamma_\infty} w(\xi)$$

where the minus sign is to be taken for the interval $(2p - 1)\pi < \xi < 2p\pi$ and the plus sign for the interval $2p\pi < \xi < (2p + 1)\pi$. For a warped wing the periodically variable incidence angle may be given in the form

$$\alpha(\xi) = \alpha_0 f(\xi) \quad \alpha_0 = \alpha \quad \text{for } \xi = 0$$

We then have:

$$\frac{\Gamma(\xi)}{\Gamma_0} \frac{1}{1 + |\sin \xi|} = \frac{f(\xi)}{1 + |\sin \xi|} - \frac{c t}{2\Gamma_0} w(\xi) \quad \left(\frac{c v t \alpha_0}{2} = \Gamma_0 \right)$$

We develop

$$\frac{1}{1 + |\sin \xi|} = \sum_0^{\infty} b_{2m} \cos 2m \xi$$

and

$$\frac{f(\xi)}{1 + |\sin \xi|} = \sum_1^{\infty} \beta_n \sin n \xi$$

The coefficients b_{2m} and β_n are obtained by analyzing harmonically the given functions:

[#]A typographical error should be pointed out; the left side of the equations on page 347 should read:

$$a_1(2b_0 + \frac{2}{\lambda} - b_2); a_3(2b_0 + \frac{6}{\lambda} - b_6); a_5(2b_0 + \frac{10}{\lambda} - b_{10}); \dots$$

$$\frac{1}{1 + |\sin \xi|} \quad \text{and} \quad \frac{f(\xi)}{1 + |\sin \xi|}$$

We then set

$$\frac{\Gamma(\xi)}{\Gamma_0} = \sum_1^{\infty} a_n \sin n \xi$$

so that

$$\frac{w(\xi)}{\Gamma_0} = \frac{1}{4} \sum_1^{\infty} a_n n \sin n \xi$$

and with $8/ct = \lambda$, obtain

$$\begin{aligned} \frac{1}{2} \sum_{n=1}^{\infty} \sum_{m=0}^{\infty} a_n b_{2m} [\sin (n + 2m) \xi + \sin (n - 2m) \xi] \\ = \sum_{n=1}^{\infty} \left(\beta_n - \frac{n}{\lambda} a_n \right) \sin n \xi \end{aligned}$$

By comparing the coefficients, the following set of equations for a_n are obtained:

$$a_1 \left(\frac{2}{\lambda} + 2b_0 - b_2 \right) = 2\beta_1 - \left[\begin{array}{cccc} & a_3(b_2 - b_4) & + a_5(b_4 - b_6) & + \dots \end{array} \right]$$

$$a_2 \left(\frac{4}{\lambda} + 2b_0 - b_4 \right) = 2\beta_2 - \left[\begin{array}{cccc} & a_4(b_2 - b_6) & + a_6(b_4 - b_8) & + \dots \end{array} \right]$$

$$a_3 \left(\frac{6}{\lambda} + 2b_0 - b_6 \right) = 2\beta_3 - \left[\begin{array}{cccc} a_1(b_2 - b_4) & & + a_5(b_2 - b_8) & + a_7(b_4 - b_{10}) \dots \end{array} \right]$$

$$a_4 \left(\frac{8}{\lambda} + 2b_0 - b_8 \right) = 2\beta_4 - \left[\begin{array}{cccc} & a_2(b_2 - b_6) & & + a_6(b_2 - b_{10}) + \dots \end{array} \right]$$

$$a_5 \left(\frac{10}{\lambda} + 2b_0 - b_{10} \right) = 2\beta_5 - \left[\begin{array}{cccc} a_1(b_4 - b_6) & & + a_3(b_2 - b_8) & + a_7(b_2 - b_{12}) \dots \end{array} \right]$$

4. Warped Wing with Variable Chord Spanning

a Circular Free Jet

This case may be solved in a similar manner to the previous one. The boundary condition in this case too is satisfied in such a manner that

$$t(\xi) = t(2\pi - \xi) \text{ and } \alpha(\xi) = -\alpha(2\pi - \xi)$$

In the ξ - η plane, therefore, the equation to be satisfied, is

$$\frac{\Gamma(\xi)}{\Gamma_0} \frac{1}{1 + |\sin \xi|} = \frac{\alpha(\xi)}{1 + |\sin \xi|} - \frac{c t(\xi) w(\xi)}{2\Gamma_0}$$

$$\left(\frac{c V \alpha_0 t_0}{2} = \Gamma_0, \quad \alpha_0 = \alpha \text{ for } \xi=0 \right. \\ \left. t_0 = t \text{ for } \xi=0 \right)$$

We develop:

$$\frac{1}{1 + |\sin \xi|} = \sum_0^{\infty} b_{2m} \cos 2m \xi$$

and

$$\frac{\alpha(\xi)}{1 + |\sin \xi|} = \alpha_0 \sum_1^{\infty} \beta_n \sin n \xi$$

Furthermore,

$$t(\xi) = t_0 \sum_0^{\infty} d_p \cos p \xi$$

which with

$$\frac{\Gamma(\xi)}{\Gamma_0} = \sum_1^{\infty} a_n \sin n \xi$$

becomes

$$\frac{w(\xi)}{\Gamma_0} = \frac{1}{4} \sum_1^{\infty} a_n n \sin n \xi$$

These relations substituted in the above equation give:

$$\frac{1}{2} \sum_{n=1}^{\infty} \sum_{m=0}^{\infty} a_n b_{2m} [\sin (n + 2m) \xi + \sin (n - 2m) \xi] \\ = \sum_{n=1}^{\infty} \beta_n \sin n \xi \\ - \frac{1}{2\lambda} \sum_{p=0}^{\infty} \sum_{n=1}^{\infty} d_p a_n n [\sin (n + p) \xi + \sin (n - p) \xi]$$

By comparing the coefficients, the following set of equations is obtained for the constants:

$$a_1 \left(2b_0 - b_2 + \frac{2d_0 - d_2}{\lambda} \right) = 2\beta_1 - \left[\begin{array}{l} a_2(d_1 - d_3) + a_3(d_2 - d_4) + a_4(d_3 - d_5) + a_5(d_4 - d_6) + \dots \\ - \left[\begin{array}{l} a_3(b_2 - b_4) \qquad \qquad + a_5(b_4 - b_6) \qquad \qquad + a_7(b_6 - b_8) + \dots \end{array} \right] \end{array} \right]$$

$$a_2 \left(2b_0 - b_4 + \frac{4d_0 - 2d_4}{\lambda} \right) = 2\beta_2 - \left[\begin{array}{l} a_1(d_1 - d_3) \qquad \qquad + a_3(d_1 - d_5) + a_4(d_2 - d_6) + a_5(d_3 - d_7) + \dots \\ - \left[\begin{array}{l} a_4(b_2 - b_6) \qquad \qquad + a_6(b_4 - b_8) + \dots \end{array} \right] \end{array} \right]$$

$$a_3 \left(2b_0 - b_6 + \frac{6d_0 - 3d_6}{\lambda} \right) = 2\beta_3 - \left[\begin{array}{l} a_1(d_2 - d_4) + a_2(d_1 - d_5) \qquad \qquad + a_4(d_1 - d_7) + a_5(d_2 - d_8) + \dots \\ - \left[\begin{array}{l} a_1(b_2 - b_4) \qquad \qquad + a_5(b_2 - b_8) \qquad \qquad + a_7(b_4 - b_{10}) + \dots \end{array} \right] \end{array} \right]$$

$$a_4 \left(2b_0 - b_8 + \frac{8d_0 - 4d_8}{\lambda} \right) = 2\beta_4 - \left[\begin{array}{l} a_1(d_3 - d_5) + a_2(d_4 - d_6) + a_3(d_1 - d_7) \qquad \qquad + a_5(d_1 - d_9) + \dots \\ - \left[\begin{array}{l} a_2(b_2 - b_6) \qquad \qquad + a_6(b_2 - b_{10}) + \dots \end{array} \right] \end{array} \right]$$

⋮

The system is solved by iteration.

5. Wing Spanning Rectangular Free Jet and Placed Eccentrically

The wing is placed across a free jet of rectangular cross section normal to the side edges (fig. 10). Let the distance from the upper boundary of the jet be s ; we then define $E = 1 - 2s/h$ as a measure of the eccentricity. The jet boundary conditions may be satisfied as follows: Assuming the fluid to extend indefinitely, let the wing lie along the X axis, and let the angle of attack change periodically from $+\alpha$ to $-\alpha$; the period is equal to $2l$ and the places where the change occurs are at $x = 0, \pm l, \pm 2l, \pm 3l, \dots$. In this manner the jet condition is satisfied at the free side boundaries. The condition for the sides parallel to the X axis may be satisfied by applying the image method. By forming a wing grating such that a wing with periodic change of angle of attack is placed at each position

$$z = 0, 2s, \pm 2h, \pm 2h+2s, \pm 4h, \pm 4h+2s, \dots$$

it is easy to see that by this arrangement the required conditions are satisfied (fig. 10).

For purposes of computation, we split this grating up into a symmetrical part, consisting of the wings at $z = 0, \pm 2h, \pm 4h, \dots$ ($0, \pm 1, \pm 2$ in fig. 10) and an unsymmetrical part, consisting of the wings at $z = 2s, \pm 2h+2s, \pm 4h+2s, \dots$ ($\pm I, \pm II, \dots$ in fig. 10). The unsymmetrical part gives the effect of the eccentricity. According to wing theory:

$$w(x) = \frac{1}{4\pi} \int_{-\infty}^{\infty} \sum_{m=-\infty}^{\infty} \frac{d\Gamma(x_1)}{dx_1} \frac{(x-x_1) dx_1}{(x-x_1)^2 + (2mh)^2} \\ + \frac{1}{4\pi} \int_{-\infty}^{\infty} \sum_{m=-\infty}^{\infty} \frac{d\Gamma(x_1)}{dx_1} \frac{(x-x_1) dx_1}{(x-x_1)^2 + \left[\left(m + \frac{1-E}{2} \right) 2h \right]^2}$$

Now (reference 3, p. 341):

$$\begin{aligned} \frac{1}{4\pi} \int_{-\infty}^{\infty} \sum_{m=-\infty}^{\infty} \frac{d\Gamma(x_1)}{dx_1} \frac{(x-x_1) dx_1}{(x-x_1)^2 + (2mh)^2} \\ = \frac{1}{8h} \int_{-\infty}^{\infty} \frac{d\Gamma(x_1)}{dx_1} \coth \frac{\pi(x-x_1)}{2h} dx_1 \end{aligned}$$

and

$$\begin{aligned} \frac{1}{4\pi} \int_{-\infty}^{\infty} \sum_{m=-\infty}^{\infty} \frac{d\Gamma(x_1)}{dx_1} \frac{(x-x_1) dx_1}{(x-x_1)^2 + \left[\left(m + \frac{1-E}{2} \right) 2h \right]^2} \\ = \frac{1}{8\pi h} \int_{-\infty}^{\infty} \sum_{m=0}^{\infty} \frac{d\Gamma(x_1)}{dx_1} \frac{\frac{x-x_1}{2h} dx_1}{\left(\frac{x-x_1}{2h} \right)^2 + \left(m + \frac{1-E}{2} \right)^2} \\ + \frac{1}{8\pi h} \int_{-\infty}^{\infty} \sum_{m=0}^{\infty} \frac{d\Gamma(x_1)}{dx_1} \frac{\frac{x-x_1}{2h} dx_1}{\left(\frac{x-x_1}{2h} \right)^2 + \left(m + \frac{1+E}{2} \right)^2} \end{aligned}$$

The periodically changing angle of attack we develop into a Fourier series:

$$\alpha(x) = \alpha^* \frac{4}{\pi} \sum_1^{\infty} \frac{\sin n \pi \frac{x}{l}}{n} \quad (n \text{ unequal})$$

and a similar series for the circulation with coefficients as yet undetermined

$$\Gamma(x) = \Gamma_{\infty} \sum_1^{\infty} a_n \sin \pi \frac{x}{l}$$

Substituting in the above equations, we obtain with

$$\frac{x-x_1}{2h} = \xi:$$

$$\begin{aligned} w(x) = \Gamma_{\infty} \sum_{n=1}^{\infty} \frac{a_n n \pi}{4l} \frac{e^{\frac{2n\pi h}{l}} + 1}{e^{\frac{2n\pi h}{l}} - 1} \sin n \pi \frac{x}{l} \\ + \frac{\Gamma_{\infty}}{8\pi h} \int_{-\infty}^{\infty} \sum_{n=1}^{\infty} \sum_{m=0}^{\infty} \frac{a_n n \pi}{l} \frac{\xi \cos n \pi \frac{x_1}{l} dx_1}{\xi^2 + \left(m + \frac{1-E}{2} \right)^2} \end{aligned}$$

$$+ \frac{\Gamma_{\infty}}{8\pi h} \int_{-\infty}^{\infty} \sum_{n=1}^{\infty} \sum_{m=0}^{\infty} \frac{a_n n \pi}{l} \frac{\xi \cos n \pi \frac{x_1}{l}}{\xi^2 + \left(m + \frac{1+E}{2}\right)^2} dx_1$$

We consider the integral

$$\begin{aligned} J &= \int_{-\infty}^{\infty} \frac{\xi \cos n \pi \frac{x_1}{l}}{\xi^2 + \left(m + \frac{1-E}{2}\right)^2} dx_1 \\ &= 2h \int_{-\infty}^{\infty} \frac{\xi \cos \frac{n\pi}{l} (x-2h\xi)}{\xi^2 + \left(m + \frac{1-E}{2}\right)^2} d\xi \\ &= 2h \cos n \pi \frac{x}{l} \int_{-\infty}^{\infty} \frac{\xi \cos 2n \pi \frac{h}{l} \xi}{\xi^2 + \left(m + \frac{1-E}{2}\right)^2} d\xi \\ &\quad + 2h \sin n \pi \frac{x}{l} \int_{-\infty}^{\infty} \frac{\xi \sin 2n \pi \frac{h}{l} \xi}{\xi^2 + \left(m + \frac{1-E}{2}\right)^2} d\xi \end{aligned}$$

Now

$$\int_{-\infty}^{\infty} \frac{\xi \cos 2n \pi \frac{h}{l} \xi}{\xi^2 + \left(m + \frac{1-E}{2}\right)^2} d\xi = 0$$

and

$$\frac{\xi \sin 2n \pi \frac{h}{l} \xi}{\xi^2 + \left(m + \frac{1-E}{2}\right)^2} d\xi = \pi e^{-2n \pi \frac{h}{l} \left(m + \frac{1-E}{2}\right)}$$

so that

$$J = 2h \pi e^{-2n \pi \frac{h}{l} \left(m + \frac{1-E}{2}\right)} \sin n \pi \frac{x}{l}$$

Thus, we finally obtain:

$$\begin{aligned}
 w(x) = & \frac{\Gamma_{\infty} \pi}{4l} \sum_{n=1}^{\infty} a_n n \frac{e^{\frac{2n\pi}{l} \frac{h}{l} + 1}}{e^{\frac{2n\pi}{l} \frac{h}{l} - 1}} \sin n \pi \frac{x}{l} \\
 & + \frac{\Gamma_{\infty} \pi}{4l} \sum_{n=1}^{\infty} \sum_{m=0}^{\infty} a_n n e^{-2n\pi \frac{h}{l} \left(m + \frac{1-E}{2}\right)} \sin n \pi \frac{x}{l} \\
 & + \frac{\Gamma_{\infty} \pi}{4l} \sum_{n=1}^{\infty} \sum_{m=0}^{\infty} a_n n e^{-2n\pi \frac{h}{l} \left(m + \frac{1+E}{2}\right)} \sin n \pi \frac{x}{l}
 \end{aligned}$$

Substituting in the well-known equation from wing theory

$$\Gamma(x) = \frac{cVt}{2} \alpha(x) - \frac{w(x)}{v} \quad \text{the Fourier series for } \Gamma(x),$$

$\alpha(x)$, and $w(x)$, we obtain with $\frac{cVt\alpha^*}{2} = \Gamma_{\infty}$ equation

$$\begin{aligned}
 \sum_{n=1}^{\infty} a_n \sin n \pi \frac{x}{l} = & \sum_{n=1}^{\infty} \left\{ \frac{4\pi}{n} - \frac{ct\pi}{8l} \left[a_n n \frac{e^{\frac{2n\pi}{l} \frac{h}{l} + 1}}{e^{\frac{2n\pi}{l} \frac{h}{l} - 1}} - \right. \right. \\
 & \left. \left. a_n n \sum_{m=0}^{\infty} \left(e^{-2n\pi \frac{h}{l} \left(m + \frac{1-E}{2}\right)} + e^{-2n\pi \frac{h}{l} \left(m + \frac{1+E}{2}\right)} \right) \right] \right\} \sin n \pi \frac{x}{l}
 \end{aligned}$$

Setting $\frac{8l}{ct\pi} = \lambda$, there is obtained by comparing coefficients,

$$a_n = \frac{4}{\pi n \left\{ 1 + \frac{n}{\lambda} \left[\frac{e^{\frac{2n\pi}{l} \frac{h}{l}} + 1}{e^{\frac{2n\pi}{l} \frac{h}{l}} - 1} + \sum_{m=0}^{\infty} \left(e^{-2n\pi \frac{h}{l} \left(m + \frac{1-E}{2}\right)} + e^{-2n\pi \frac{h}{l} \left(m + \frac{1+E}{2}\right)} \right) \right] \right\}}$$

$$= \frac{4}{\pi n \left\{ 1 + \frac{n}{\lambda} \left[\frac{1 + e^{-2n\pi \frac{h}{l}}}{1 - e^{-2n\pi \frac{h}{l}}} + \left(e^{-2n\pi \frac{h}{l} \frac{1-E}{2}} + e^{-2n\pi \frac{h}{l} \frac{1+E}{2}} \right) \sum_{m=0}^{\infty} e^{-2n\pi m \frac{h}{l}} \right] \right\}}$$

It turns out that it is sufficient to consider the first two terms only of the series obtained by the division

$$\frac{1 + e^{-2n\pi \frac{h}{l}}}{1 - e^{-2n\pi \frac{h}{l}}} \text{ as well as the first two terms of the sum } \sum_{m=0}^{\infty} e^{-2n\pi m \frac{h}{l}}$$

In this way there is obtained:

$$a_n = \frac{4}{\pi n \left\{ 1 + \frac{n}{\lambda} \left[1 + 2e^{-2n\pi \frac{h}{l}} + \left(e^{-2n\pi \frac{h}{l} \frac{1-E}{2}} + e^{-2n\pi \frac{h}{l} \frac{1+E}{2}} \right) \left(1 + e^{-2n\pi \frac{h}{l}} \right) \right] \right\}}$$

TABLE II

E	λ	$x/l =$			
		0.5	0.25	0.125	0.0625
0.75	1	0.442	0.398	0.321	0.235
	2	.620	.576	.484	.355
	3	.717	.671	.583	.458
	4	.773	.752	.652	.528
	5	.808	.772	.701	.578
	6	.835	.803	.739	.615
	7	.856	.827	.770	.655
	8	.875	.844	.794	.682
	9	.887	.860	.815	.706
0.5	1	0.510	0.454	0.337	0.242
	2	.669	.618	.505	.380
	3	.756	.710	.609	.470
	4	.806	.766	.677	.535
	5	.841	.804	.724	.589
	6	.865	.832	.758	.631
	7	.881	.851	.789	.665
	8	.895	.867	.810	.692
	9	.906	.880	.828	.715
0.25	1	0.524	0.465	0.347	0.246
	2	.695	.624	.510	.381
	3	.776	.725	.673	.472
	4	.826	.782	.679	.537
	5	.856	.817	.728	.590
	6	.879	.843	.762	.632
	7	.895	.862	.793	.667
	8	.907	.878	.813	.695
	9	.916	.888	.831	.719
0	1	0.531	0.470	0.352	0.248
	2	.702	.634	.513	.382
	3	.784	.733	.616	.474
	4	.831	.790	.682	.539
	5	.860	.823	.730	.592
	6	.883	.853	.765	.633
	7	.898	.869	.795	.667
	8	.910	.885	.815	.695
	9	.920	.896	.833	.720

As an example, the computation was carried out for the square section jet ($\frac{h}{l} = 1$). The eccentricities chosen were $E = 0.25, 0.5, \text{ and } 0.75$. Integral values of λ were used from 1 to 9, which included all aspect ratios of practical interest. Figures 11, 12, 13, and 14 show the circulation at different points of the wing as functions of λ . The computed values are given in table II where, for comparison, are also given the values for the wing lying across the middle of the jet ($E = 0$). Figure 15 gives the circulation over the wing at the different degrees of eccentricity.

From the computed distribution of the circulation the total lift A of a wing at different eccentricities was determined. The quotient of these values by A_0 , the value with wing spanned across the middle of the jet, shows up the effect of the eccentricity (fig. 16). It is seen from the figure that the effect of the eccentricity between $E = 0$ to $E = 0.5$, which is the range that is of practical interest, is only very slight. For comparison, the values of A/A_0 were determined when the height of the jet, with the wing spanning its middle, was reduced from $h = l$ to $h = 0$ (fig. 17). It is easily seen that this narrowing of the jet does have a strong effect on the wing lift.

6. Wing Spanning a Free Jet of Circular Cross Section Eccentrically

For a wing spanning a circular jet eccentrically, the above method of computation is not applicable. A solution may be obtained, however, in the following manner. Considering the relations at an infinite distance behind the wing, the jet condition for the circular boundary may be satisfied by the method of images, using reciprocal radii (fig. 18). A circulation approximating the actual distribution is first assumed and from it the induced downward velocities produced by the wing itself and the images are computed. These velocities together with the assumed distribution of circulation allow the geometric angles of incidence to be determined along the span. By suitably changing the circulation distribution, the angles of incidence thus derived are made to agree with the given values. This process is rather complicated and not absolutely reliable. It thus appeared desirable to solve this problem experimentally.

II. EXPERIMENTAL PART

To supplement the theoretical investigations described above, certain tests were carried out. The problem was to determine the effect of eccentric positioning on a wing spanning a free jet of circular cross section. Figure 19 shows the test apparatus. The wing, spanning a 40-centimeter-diameter jet, is suspended on two scales to determine its lift and drag. Three wings with profile Göttingen 398 and chords of 5, 10, and 20 centimeters, respectively, were tested. The relative velocity was about 30 meters per second. The polars of these models obtained in the Göttingen wind tunnel are shown on figure 20. All wings were 70 centimeters long.

The axis which defines the position of the wing is shown in figure 21. The position of this axis practically coincides with the mean pressure line of the wing, since it seems reasonable from theoretical considerations that this position coincides with the position of the vortex filament. The angle of attack of the wing was likewise taken with respect to this axis.

In all the tests the distance of the wing from the throat of the tunnel (d) was taken equal to $0.3 R$. Beyond this position the static pressure in the jet was constant, and the mixing zone at the jet boundary of small extent. In order to study the effect of distance of the wing from the plane of the tunnel outlet, the drag and lift were measured for a wing ($R/t = 2$) placed at 6° angle of attack at various distances from the throat. The measured values were made dimensionless by dividing by the values obtained at the position $d = 0.3 R$. The results are shown in figure 22. It may be seen that the lift is almost completely independent of the distance d/R . The drag, however, increases with distance from tunnel throat. With increasing distance, the effect of the throat on the down flow decreases; moreover, the lift distribution becomes less favorable. As the jet broadens out, larger portions of the wing surface are exposed to the jet while the jet velocity decreases. The effect of each factor is not known separately, but their combined effect brings about the increased drag mentioned above.

$$\text{cm} \times 0.3937 = \text{in.} \quad \text{m/s} \times 3.28083 = \text{ft./sec.}$$

TABLE III

α°	E = 0		0.2		0.4		0.6		0.8	
	C_a	C_w								
R/t = 4										
-18	-0.353	0.208	-0.335	0.201	-0.312	0.196	-0.297	0.198	-0.276	0.199
-15	-.330	.165	-.315	.160	-.292	.157	-.275	.152	-.255	.149
-12	-.298	.125	-.280	.120	-.261	.116	-.244	.114	-.225	.110
-9	-.230	.083	-.215	.080	-.200	.078	-.182	.075	-.165	.072
-6	-.027	.028	-.025	.028	-.023	.028	-.020	.028	-.018	.028
-3	.198	.018	.185	.019	.170	.020	.150	.021	.125	.023
0	.398	.024	.382	.026	.355	.027	.323	.028	.275	.029
3	.589	.035	.580	.038	.549	.039	.493	.042	.425	.045
6	.770	.051	.753	.052	.718	.057	.659	.061	.584	.065
9	.941	.072	.932	.078	.891	.081	.830	.086	.726	.088
12	1.090	.103	1.064	.106	1.042	.111	.971	.117	.870	.122
15	1.155	.135	1.145	.139	1.136	.143	1.088	.152	1.029	.167
18	1.112	.192	1.111	.193	1.076	.197	1.048	.206	.995	.219
21	.920	.320	.931	.320	.892	.322	.841	.325	.795	.348
R/t = 2										
-18	-0.254	0.171	-0.260	0.168	-0.264	0.166	-0.271	0.165	-0.275	0.165
-15	-.240	.136	-.246	.135	-.252	.135	-.256	.133	-.264	.132
-12	-.195	.098	-.207	.097	-.212	.096	-.217	.094	-.219	.091
-9	-.100	.042	-.104	.041	-.108	.039	-.114	.038	-.118	.037
-6	.033	.015	.032	.016	.023	.017	.020	.018	.015	.019
-3	.172	.010	.168	.012	.155	.014	.150	.017	.125	.022
0	.311	.020	.310	.021	.305	.024	.280	.026	.245	.031
3	.442	.035	.435	.036	.422	.037	.396	.039	.360	.044
6	.580	.052	.575	.054	.558	.056	.520	.058	.475	.061
9	.724	.074	.711	.076	.692	.080	.650	.084	.591	.086
12	.853	.098	.842	.102	.820	.105	.762	.109	.710	.119
15	.970	.130	.955	.132	.933	.134	.870	.141	.815	.154
18	1.075	.190	1.060	.198	1.045	.204	.980	.208	.895	.210
21	1.082	.230	1.072	.232	1.057	.236	1.004	.244	.930	.264

TABLE III (Continued)

		E = 0		0.2		0.4		0.6		0.8	
α°		C_a	C_w								
R/t = 1	-18	-0.228	0.133	-0.232	0.135	-0.242	0.140	-0.254	0.141	-0.268	0.144
	-15	-.186	.088	-.188	.089	-.200	.089	-.205	.091	-.210	.092
	-12	-.125	.045	-.130	.047	-.135	.048	-.144	.049	-.153	.052
	-9	-.044	.017	-.055	.019	-.066	.020	-.075	.023	-.086	.026
	-6	.039	.004	.030	.005	.015	.008	-.007	.013	-.028	.020
	-3	.121	.007	.114	.010	.096	.012	.061	.016	.024	.020
	0	.208	.018	.190	.018	.178	.020	.142	.023	.094	.027
	3	.294	.032	.283	.033	.263	.033	.222	.035	.159	.037
	6	.369	.048	.352	.048	.339	.049	.305	.051	.232	.052
	9	.454	.071	.444	.072	.428	.073	.394	.076	.322	.078
	12	.534	.096	.521	.097	.506	.099	.475	.103	.403	.106
	15	.610	.125	.604	.128	.581	.130	.548	.135	.489	.140
	18	.690	.158	.680	.164	.651	.165	.613	.169	.560	.178
	21	.759	.192	.745	.196	.725	.204	.690	.212	.632	.220

The results of the tests are given in table III. Denoting the distance of the wing from the jet axis by a , the eccentricity $E = a/R$. In the equations $c_a = \frac{A}{qF}$ and $c_w = \frac{W}{qF}$, the area F is taken to be the area of the wing intercepted by the jet, so that $F = 2R t \sqrt{1 - E^2}$. The polars are shown in figures 23, 24, and 25, and the change of c_a with angle of attack in figures 26, 27, and 28. Due to the choice of reference axis the position of the leading edge of the wing is changed with change in angle of attack, the change being greatest, naturally, for the wing with greatest chord. This explains the peculiar shape of the lift curve at large negative angles of attack (for $R/t = 2$ and 1), the lift coefficients increasing with increasing eccentricity instead of decreasing as might be expected.

In order to obtain more general data for the wing spanning the circular jet eccentrically, the derivative $\frac{dc_a}{d\alpha}$ was obtained from the measurements as a function of λ (fig. 29). It may be seen that in this case, too, as in the case of the rectangular jet, the effect of eccentricity is very small. The effect of the eccentricity even at the highest value used in the wind tunnel ($E = 0.5$) could be applied as a correction to the computations for the wing placed along the middle of the jet.

A few more tests were carried out, finally, on a free jet of square cross section to test the validity of the theory given above. The lift on two eccentrically placed wings ($t = 5$ and 10 cm) was measured. The lift coefficients as functions of the angle of attack are shown in figures 30 and 31. In figure 32 the continuous lines give the theoretically computed values of $\frac{dc_a}{d\alpha}$, while the small circles indicate the test values. For aspect ratio $l/t = 6$, the agreement is very good; the deviations for $l/t = 3$ is explained by the fact that the distribution of the lift over the wing chord was neglected, which is not admissible for wings of such small aspect ratios.

Translation by S. Reiss,
National Advisory Committee
for Aeronautics.

REFERENCES

1. Seiferth, R., and Betz, A.: Untersuchung von Flugzeugmodellen im Windkanal. Handbuch der Experimentalphysik IV, p. 189.
2. Prandtl, L.: Tragflügeltheorie. Neudruck in L. Prandtl und A. Betz, Vier Abhandlungen zur Hydrodynamik und Aerodynamik. Göttingen, 1927, p. 55.
3. Stüper, J.: An Airfoil Spanning an Open Jet. T.M. No. 723, N.A.C.A., 1933.
4. Pistoiesi, E.: Sull'ala traversante un getto libero. Atti della Pontificia Accademia delle Scienze, Nuovi Lincei, 1933, p. 405.
5. Glauert, H.: Lift and Drag of a Wing Spanning a Free Jet. R. & M. No. 1603, British A.R.C., 1934.
6. Blenk, H., and Fuchs, O.: Druckmessungen an einem durch einen Luftstrahl hindurchgesteckten Tragflügel. D.V.L. Yearbook, 1931.

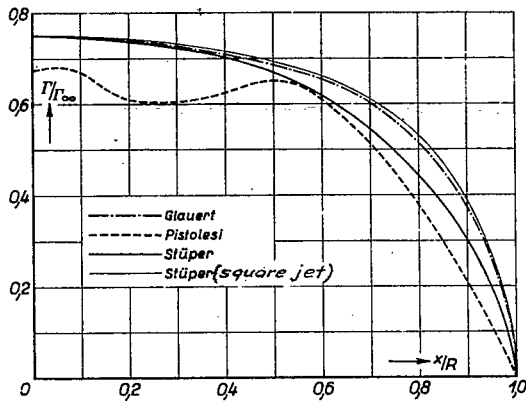


Figure 1.- Distribution of circulation about a wing spanning a circular jet.

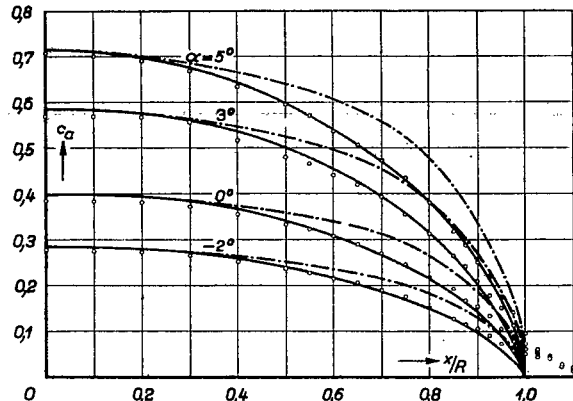


Figure 2.- Distribution of lift with circular jet.

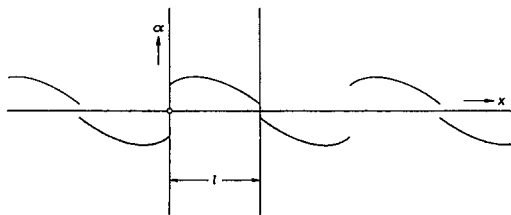


Figure 4.- Periodic variation in angle of attack.

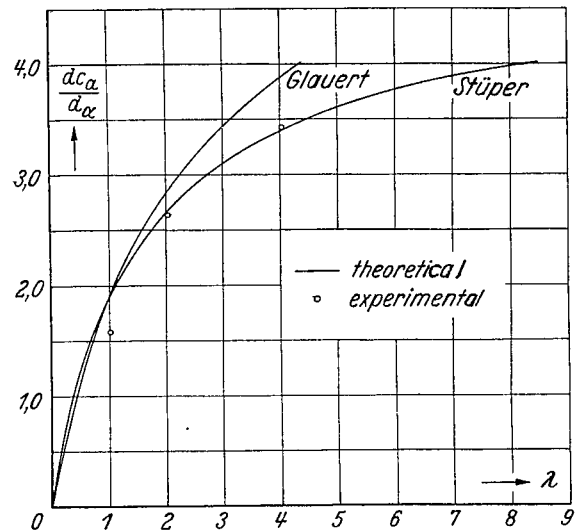


Figure 3.- Coefficient $dc_a/d\alpha$ plotted against λ .

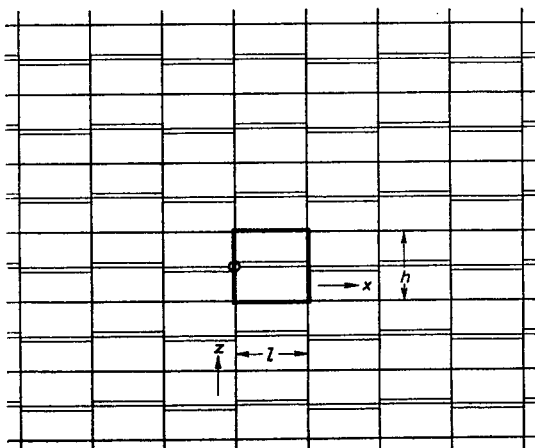


Figure 5.- Image scheme for rectangular jet.

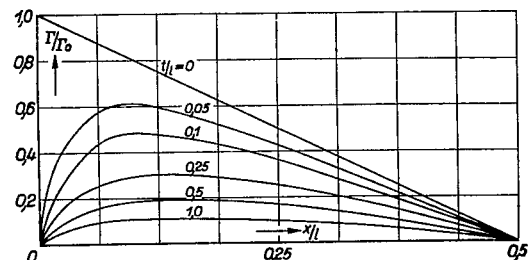


Figure 7.- Distribution of circulation of a linearly warped wing spanning a square free jet.

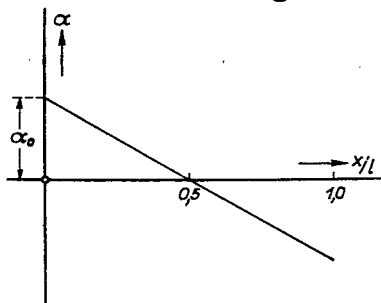


Figure 6.- Warping of the wing.

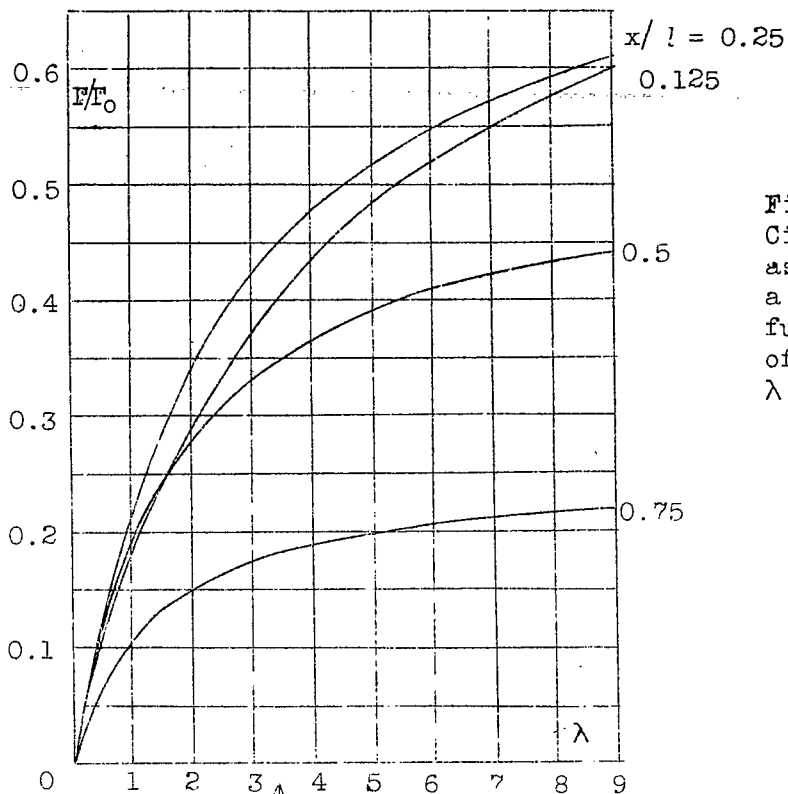


Figure 8.-
Circulation
as
a
function
of
 λ .

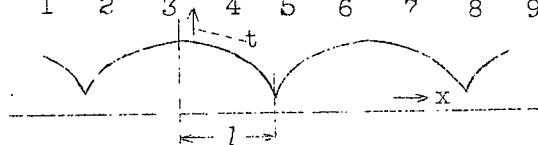


Figure 9.-
Periodic
variation
of chord.

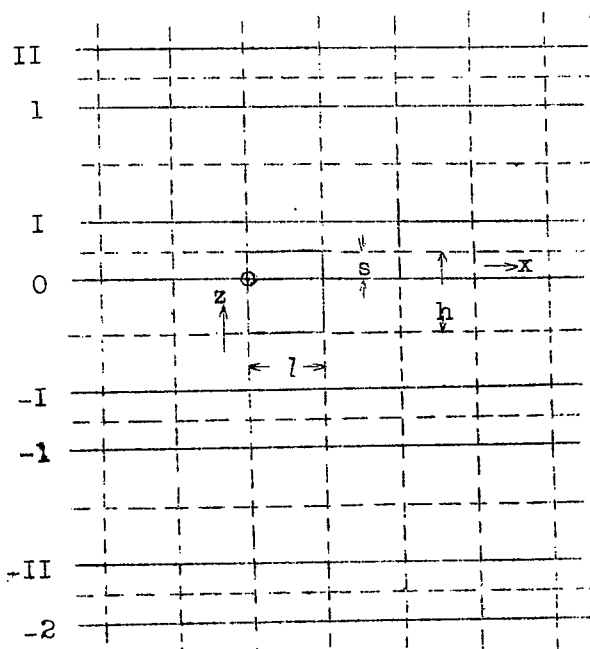


Figure 10.-
Image
scheme
for
wing
spanning
rectangular
jet
eccentrically.

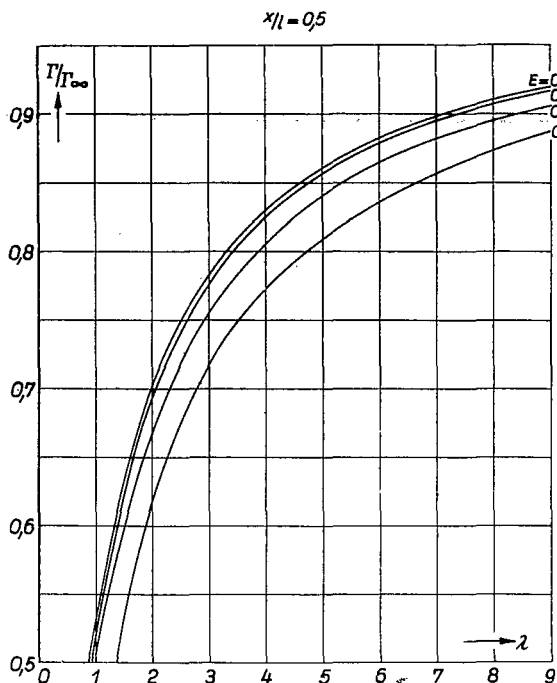


Figure 11.- Circulation with wing placed in middle of jet as a function of λ .

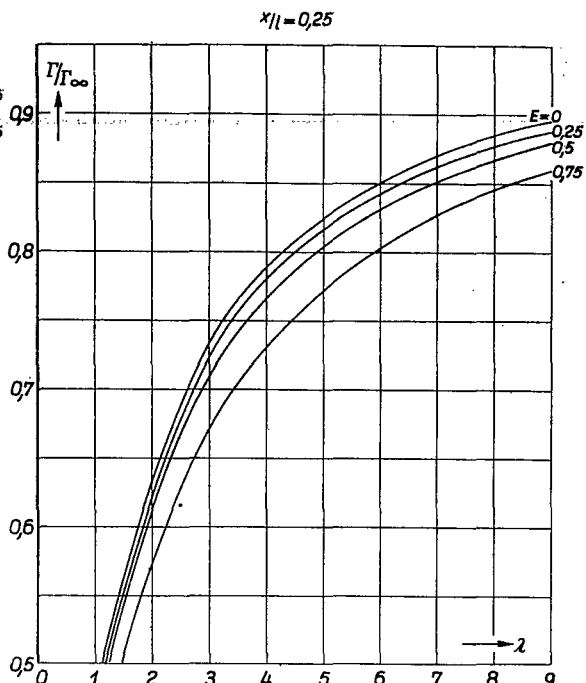


Figure 12.- Circulation with $x/l = 0,25$ as a function of λ .

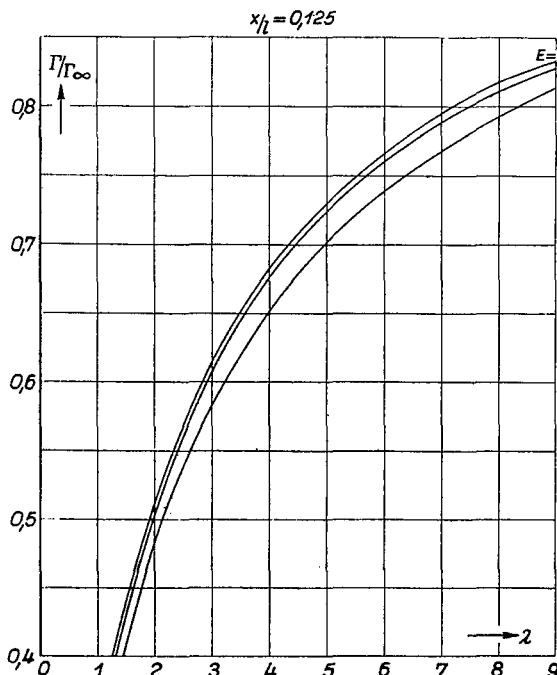


Figure 13.- Circulation with $x/l = 0,125$ as a function of λ .

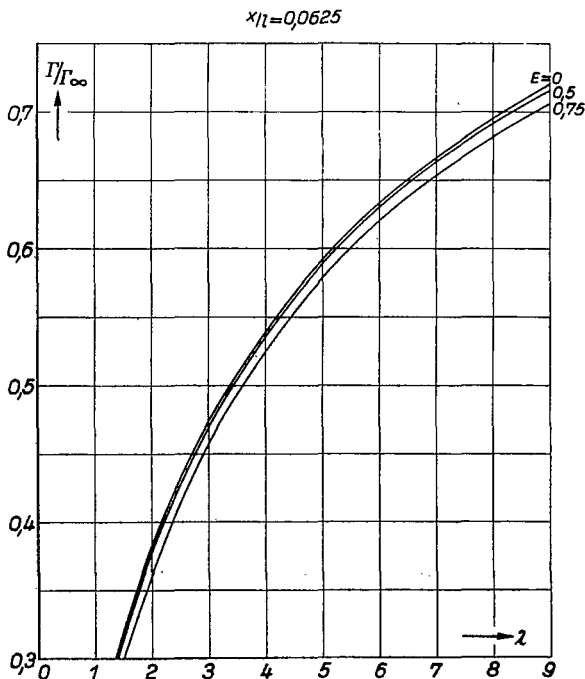


Figure 14.- Circulation with $x/l = 0,0625$ as a function of λ .

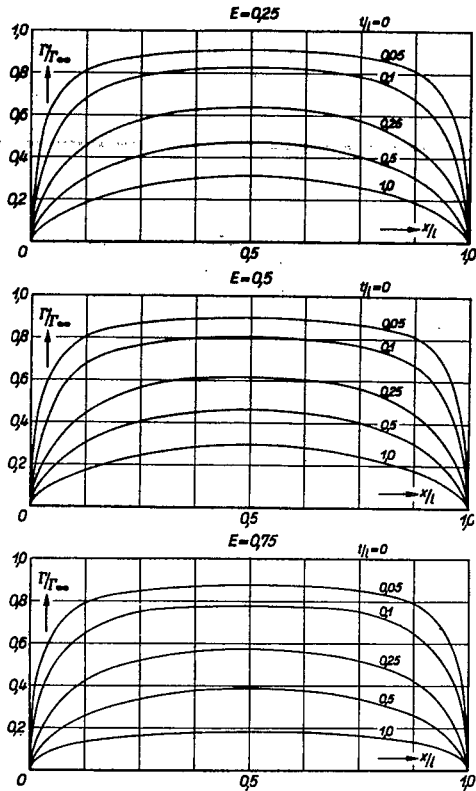


Figure 15.- Distribution of circulation of airfoil spanning a square free jet eccentrically.

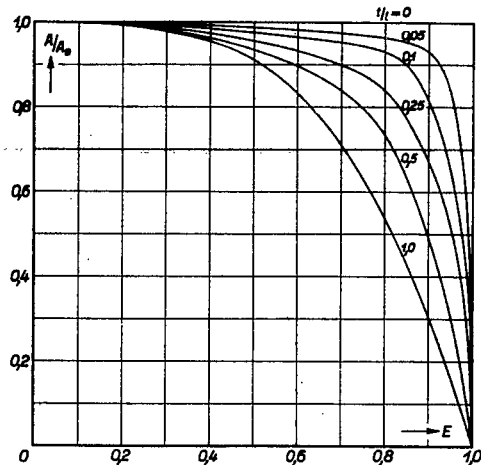


Figure 16.- Effect of eccentricity on lift.

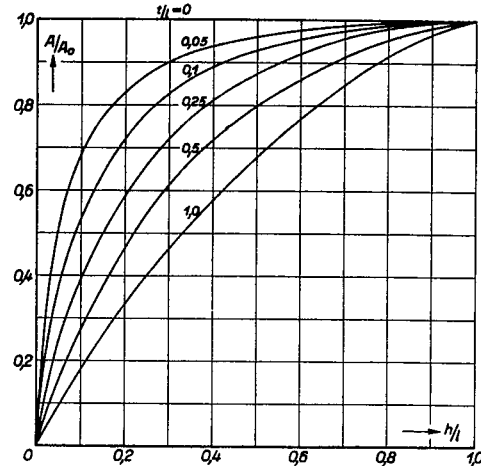


Figure 17.- Effect of decreasing jet height on lift.

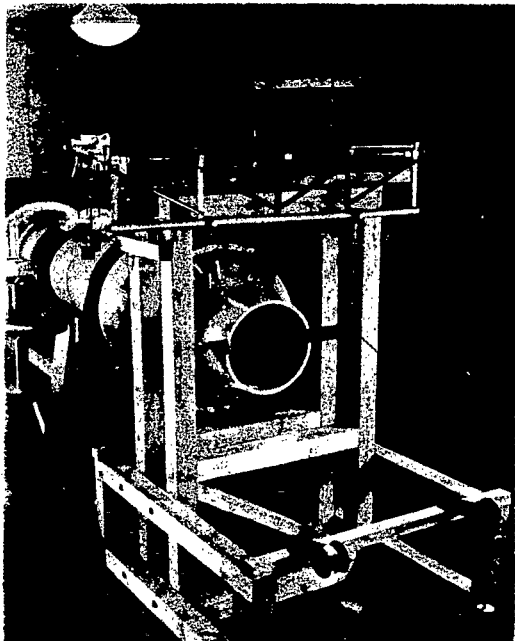


Figure 19.- Apparatus for free jet measurements.

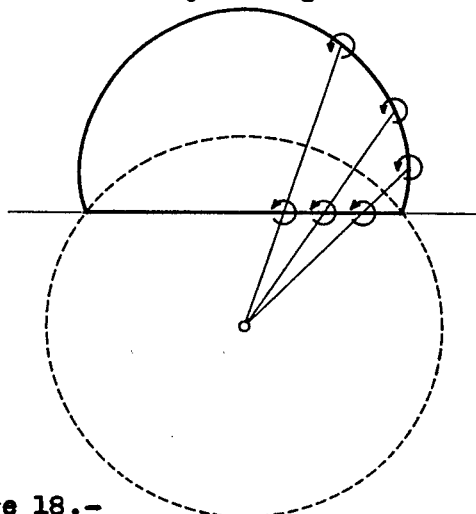


Figure 18.- Image formation for airfoil spanning circular jet eccentrically.

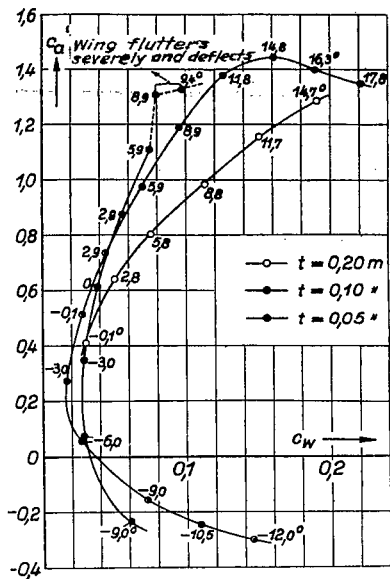


Figure 20.- Polars of the three airfoil models, profile Göttingen 398.

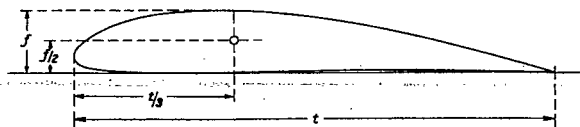


Figure 21.- Position of reference axis.

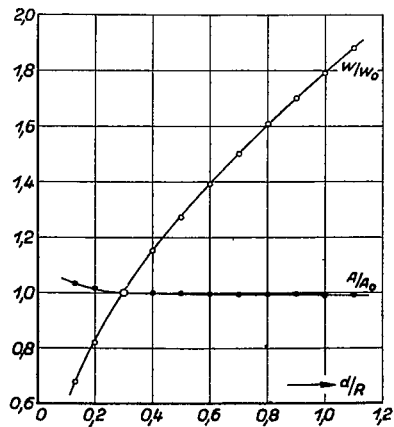


Figure 22.- Effect of distance of wing from throat of tunnel on lift and drag.

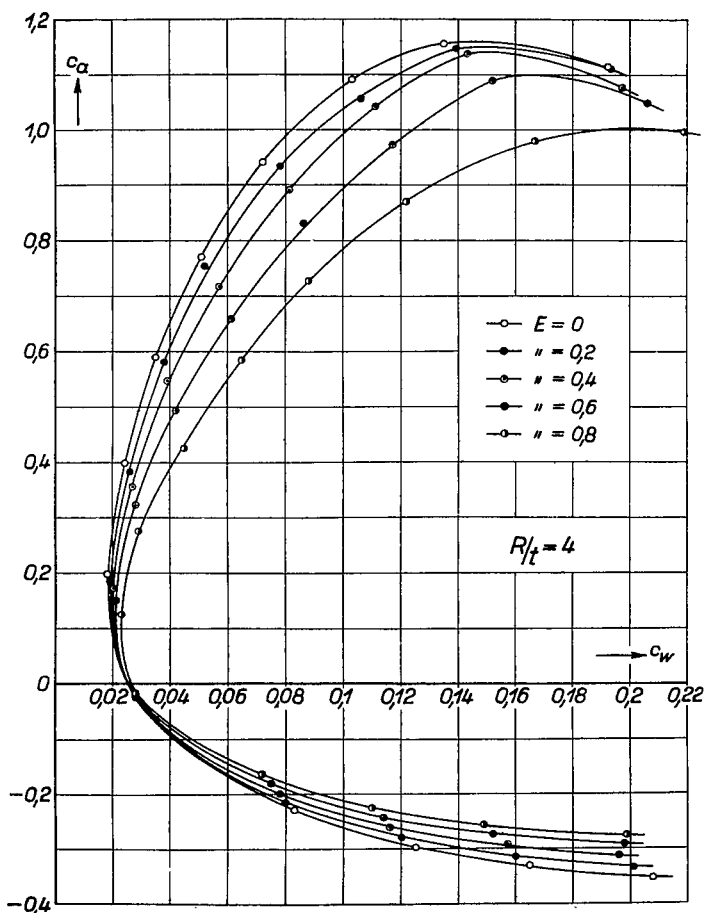


Figure 23.- Polars of wing spanning a circular free jet eccentrically, $R/t = 4$.

Figure 24.-
Polars of
wing
spanning
a circular
free jet
eccentrically,
 $R/t = 2$.

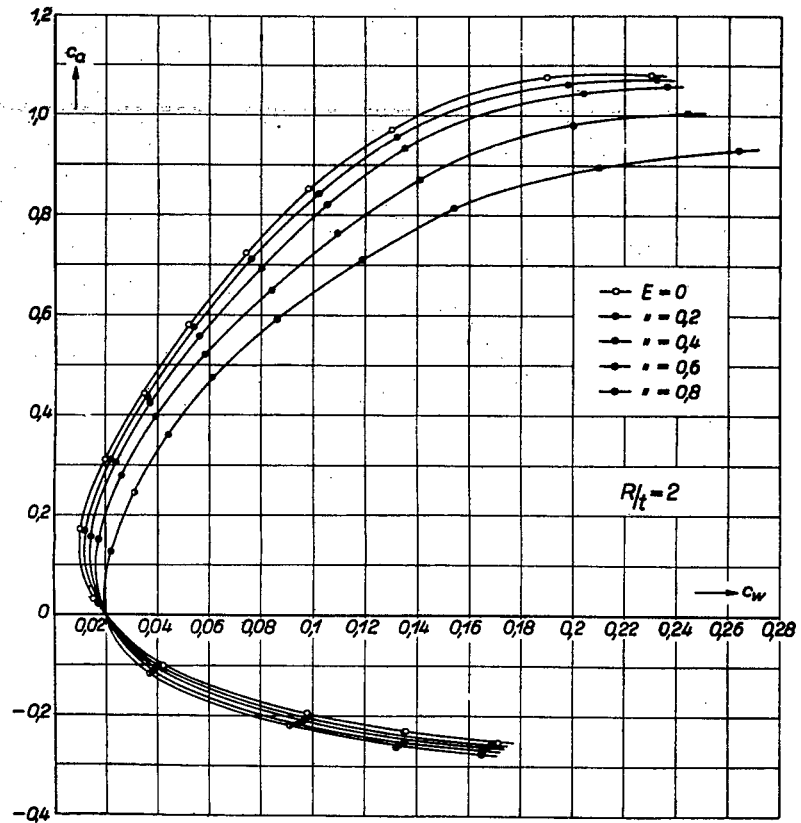
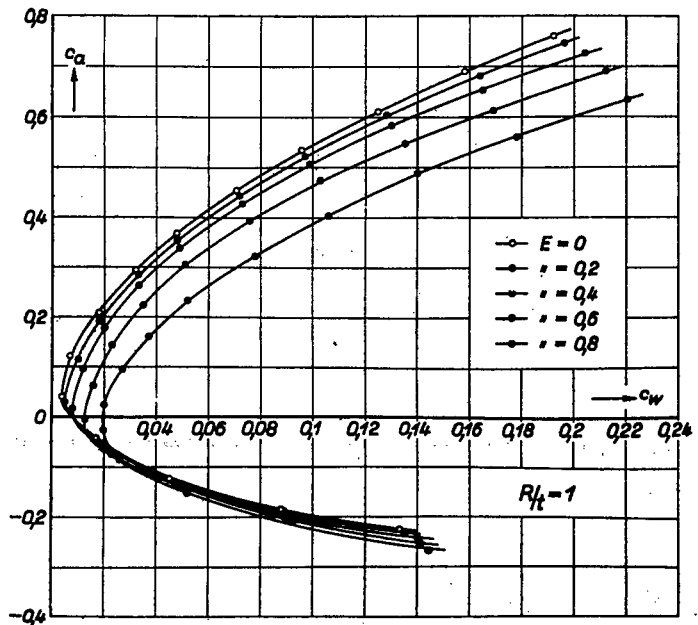


Figure 25.-
Polars of
wing
spanning
a circular
free jet
eccentrically,
 $R/t = 1$.



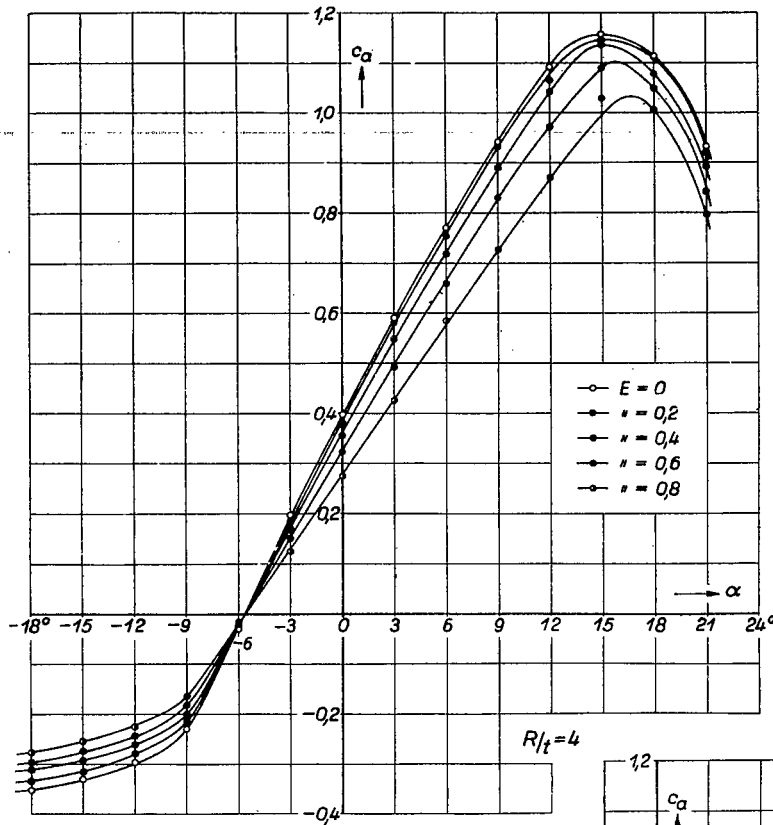


Figure 26.-
Lift
coefficient
as a function
of angle
of attack,
 $R/t = 4$.

Figure 27.-
Lift
coefficient
as a function
of angle
of attack,
 $R/t = 2$.

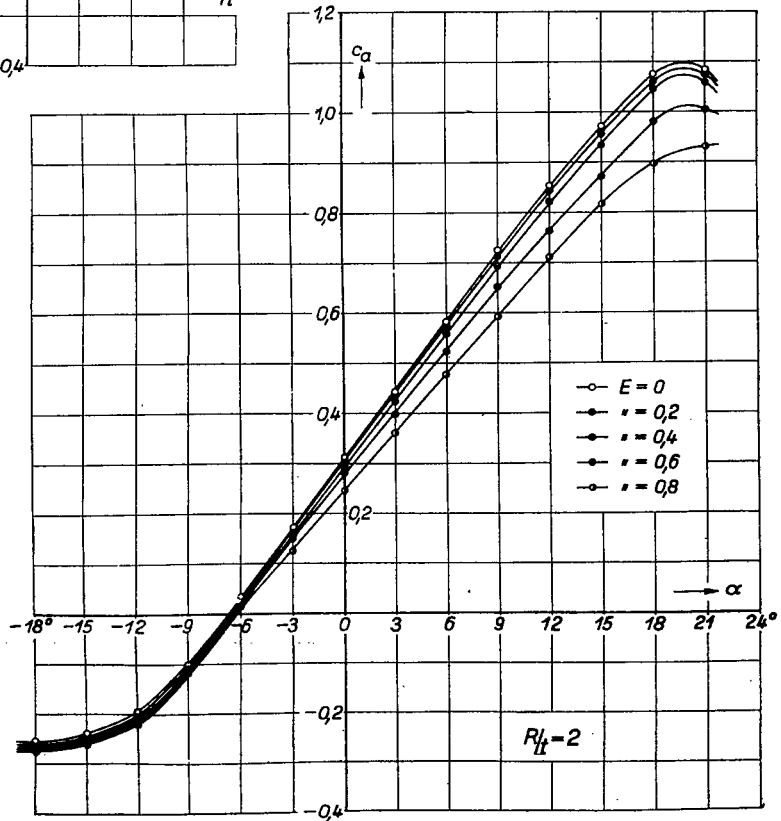


Figure 28.-
Lift
coefficient
as a function
of angle
of attack,
 $R/t = 1$.

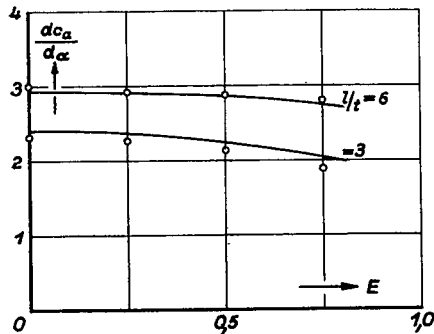
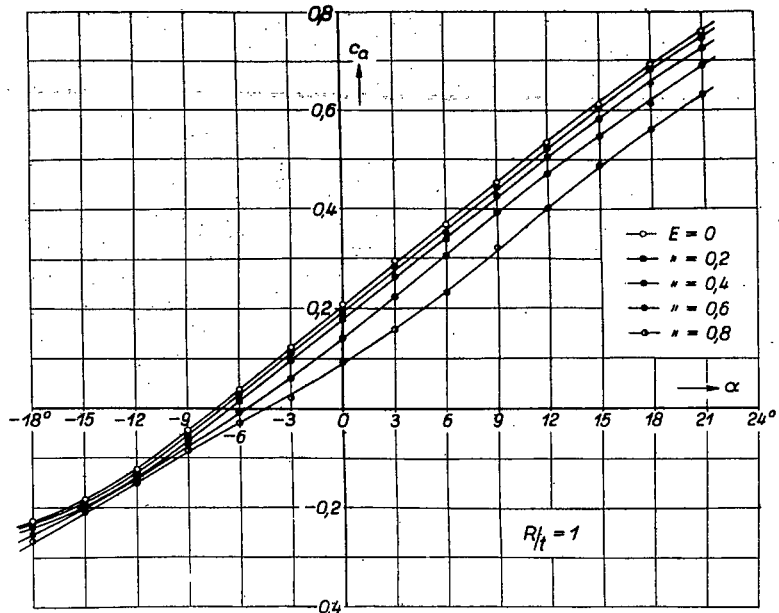


Figure 32.- Theoretical and
experimental
values of coefficient
 $dC_L/d\alpha$ for square free jet.

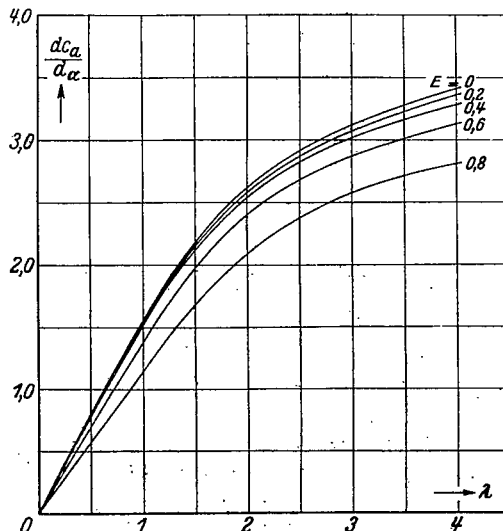


Figure 29.- Variation of coefficient
 $dC_L/d\alpha$ for wing spanning
a circular jet eccentrically.

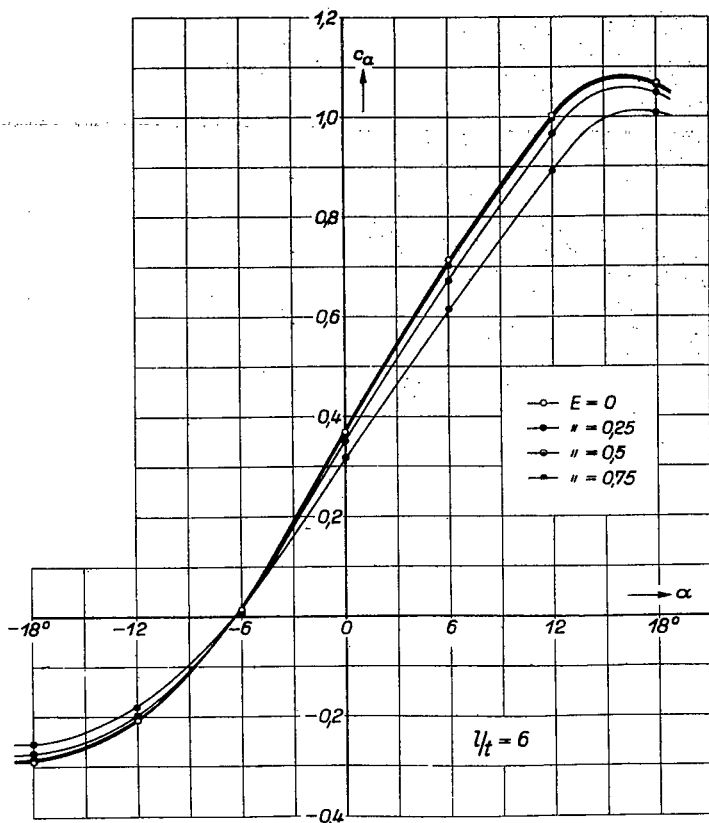
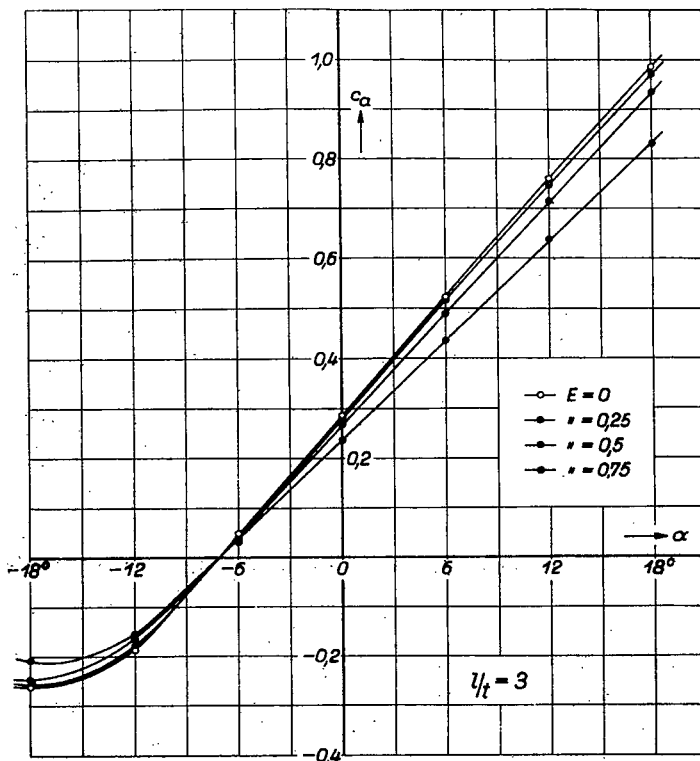


Figure 30.-
Values
of lift
coefficients
for wing
spanning
a square jet
eccentrically,
aspect ratio
($l/t = 6$).

Figure 31.-
Values
of lift
coefficients
for wing
spanning
a square jet
eccentrically,
 $l/t = 3$.



NASA Technical Library



3 1176 01441 1715